X-ray Diffraction Study of iPP/clay and iPP/TiO_2 Composites Relating to Micromechanical Properties

M. E. Cagiao,[1] F. J. Baltá Calleja,[1] F. Spieckermann,[2] S. Scholtyssek,[3] M. F. Mina,[4] M. A. H. Bhuiyan[4]

[1]*Department of Macromolecular Physics, Instituto de Estructura de la Materia, CSIC, 28006 Madrid, Spain*
[2]*Research Group Physics of Nanostructured Materials, Faculty of Physics, University of Vienna, Boltzmanngasse 5, A-1090 Vienna, Austria*
[3]*Institute of Physics, Martin-Luther University Halle-Wittenberg, D-06099, Germany*
[4]*Department of Physics, Faculty of Engineering, Bangladesh University of Engineering and Technology, Dhaka-1000, Bangladesh*

Received 9 March 2011; accepted 19 April 2011
DOI 10.1002/app.34716
Published online 4 November 2011 in Wiley Online Library (wileyonlinelibrary.com).

ABSTRACT: Composites of isotactic polypropylene with various contents of white clay or titanium dioxide TiO_2 were prepared by extrusion molding. The extruded composites were melt-pressed at two different temperatures, and, thereafter, either slowly cooled, or quenched to room temperatures. It is shown that the structure of all the samples, as revealed by wide-angle X-ray scattering and small-angle X-ray scattering (SAXS), depends on the processing conditions. The lack of SAXS maxima in the composites suggests that the presence of the microadditives hinders the stacking of iPP lamellae. Furthermore, the microindentation hardness H in the slowly cooled composites is influenced by the type and amount of the filler used. However, in the quenched samples H depends only on the amount of the filler used, and not on its type. In case of the quenched iPP/clay composites, the relationship between H and the Young's modulus E is found to be $H/E \approx 0.12$, in good agreement with Struik's theoretical predictions of $\sigma_e \approx E/30$, in consonance with results previously obtained for a series of polyethylene samples with different morphology.
 J Appl Polym Sci 124: 3147–3153, 2012

Key words: composites; WAXS; SAXS; calorimetry; mechanical properties; hardness

INTRODUCTION

Composites made of polymers with inorganic materials as fillers have comprehensive properties, and are commonly used in many fields of industry.[1–3] Different polymers are used as matrices to prepare composites, that is, polyethylene,[4–6] polypropylene,[7] polystyrene,[8] poly(vinyl alcohol),[9] PET,[10] and so forth. On the other hand, among the inorganic materials employed as fillers in the preparation of composites, or even, nanocomposites, we can find talc,[7,11] calcium carbonate $CaCO_3$,[12] silicon dioxide SiO_2,[13] clay,[7] titanium dioxide TiO_2,[4] barium sulfate $BaSO_4$,[5] magnetite,[9] or even metals, as copper[6] or nickel[8] in the form of powder.

The presence of inorganic fillers notably alters the electrical, thermal, and mechanical properties of the pristine polymers. These properties are affected by the degree of dispersion of the filler in the polymeric matrix, and also, by the interaction between both components.

Among the thermoplastic polymers, the isotactic polypropylene iPP has found a great variety of uses. This is a low cost and easily crystallizable polymer, which makes of it a good candidate for the preparation of composites with inorganic fillers. Thus, composites of iPP with talc,[7,11] $CaCO_3$,[12] SiO_2,[13] clay,[14–16] or TiO_2,[17,18] among others, have been prepared and their resulting properties analyzed.

In this work, we present a comparative study performed on the iPP/clay and iPP/TiO_2 composites prepared with quite high filler contents (up to 50 wt %). Preceding studies on these composites had been carried out previously.[14,17,18] In addition, the nanostructure and micromechanical properties of reversibly crosslinked iPP/clay nanocomposites have been recently reported.[19,20]

The aim of this article is to investigate the influence of the filler type (i.e., clay or TiO_2), the filler content, and the sample preparation method on the structure and properties (thermal and mechanical) of the final product.

Correspondence to: F. J. B. Calleja (embalta@iem.cfmac.csic.es).

Contract grant sponsor: Spanish Ministry of Science and Innovation (MICINN); contract grant numbers: FIS2010-18069, MAT2009-00789.

Contract grant sponsors: Alexander von Humboldt Foundation, Germany, EC Research Infrastructure (FP6 Program) (Desy Project II-07-031 EC).

EXPERIMENTAL

Materials

Isotactic polypropylene iPP Cosmoplene H101E (density = 0.9 g/cm^3) supplied by The Polyolefin Company (Singapore) was used in this study. For the preparation of the composites, white clay WC from the deposits of Bijoypur, Netrakona (Bangladesh), and TiO_2 powder (particle size less than 0.2 μm) obtained in Dhaka (Bangladesh), were employed.

Sample preparation

iPP/clay composites

The clay powder was grinded and sieved, and the particle size obtained was equal to or less than 75 μm. The mixture of iPP and clay was once molded by an extruder. The extruded material was cut in small pieces. The composites were prepared by two different methods:

a. Some extruded pieces were injected in a square shaped dice, which was kept in a hot-press machine and pressed at 180°C. The melt was cooled fast by circulation of water. From the cooled composites, small rectangular pieces were prepared.
b. Another set of extruded pieces were placed in a specially designed die, heated at 165°C and pressed by a hydraulic press machine. These samples were slowly cooled in an ambient condition.

The concentrations of the clay in the samples were 0, 10, 20, 30, 40, and 50 wt %. The samples were respectively, labeled as PP0, PPC1, PPC2, PPC3, PPC4, and PPC5. Samples that were subjected to the fast cooling, that is, quenched samples, are indicated by a "Q" after the name. For instance, PPC1Q indicates the quenched sample that contains 10 wt % of clay.

iPP/TiO_2 composites

The TiO_2 particle size was less than 0.2 μm. The fabrication procedure of these composites is similar to those described in "iPP/clay composites" section. The TiO_2 concentrations in the samples were 10, 20, 30, 40, and 50 wt %. The samples were labeled as PPT1, PPT2, PPT3, PPT4, and PPT5. Similar to the iPP/clay composites, a "Q" after the name refers to the samples that were quenched.

In what follows, we will refer to the additive content (in %) by the symbol ϕ.

Here, it is convenient to stress that, since the melting point of the iPP is about 170°C (see the "Results" section below), a small increase of the processing temperature up to 180°C is not expected to influence oxidation and bond breaking considerably. In fact, the hardness values and melting temperatures shown by the polymer, both pure and in the composites with the additive, are very similar to the ones reported in the bibliography.[11,16]

Techniques

The composites were studied by wide- and small-angle X-ray scattering (WAXS and SAXS), differential scanning calorimetry (DSC), and microindentation hardness measurements.

The WAXS and SAXS experiments were performed at the A2 beamline of HASYLAB (synchrotron DESY, Hamburg). The wavelength used was $\lambda = 0.15$ nm, and the distance between the sample and the SAXS detector was 2.956 m. The angular range covered in the WAXS experiments was 5–35 2θ (°). The X-ray crystallinity (α_{WAXS}) of each sample was determined as the ratio of the area of all the crystalline peaks to the total area of the diffractogram.

The thermal study was carried out with a Perkin–Elmer (Norwalk, CT) DSC-7 differential scanning calorimeter (DSC) in an inert N_2 atmosphere. Samples weights were 5–10 mg. The temperature range studied was 40–220°C. The heating rate was 10°C/min. The DSC crystallinity (α_{DSC}) of each sample was derived from the melting enthalpy measured by DSC according to the expression: $\alpha_{DSC} = \Delta H_m / \Delta H_m^\infty$, where ΔH_m and ΔH_m^∞ are the experimental melting enthalpy and the melting enthalpy for an infinitely thick crystal, respectively.

Microindentation hardness H was measured at ambient temperature using a Leitz (Wetzlar, Germany) microindentation tester equipped with a square-based diamond indenter. The H value was derived from the residual projected area of indentation according to the following expression: $H = kP/d^2$,[21] where d is the length of the impression diagonal (m), P is the contact load applied (N), and k is a geometrical factor equal to 1.854. A load of 1 N was applied. The loading cycle was 0.1 min. Between 8 and 10 indentations were performed on the surface of each sample, and the results were averaged.

RESULTS

SAXS study

Only the iPP samples without additive prepared by the two techniques (PP0 and PP0Q) showed a maximum in the SAXS diagram. The long spacing values derived from these maxima are:

PP0: $L = 32.2$ nm.
PP0Q: $L = 18.3$ nm.

The iPP-clay and TiO_2 composites do not show any SAXS maxima, suggesting that the presence of microadditives perturbs the packing of the iPP lamellae, preventing the formation of stacks.

WAXS study

The diffractograms of, both, the slowly cooled and quenched iPP pure samples show the characteristic reflections of the α-form,[22] that is, peaks at 14.1, 16.8, 18.4, 21.0, and 21.7 (a not well-resolved doublet), 25.5, 27.5, and 29.1° of 2θ. Also, a small contribution of the γ-form appears (the peak at about 19.6–19.7° of 2θ)[22] [see Fig. 1(a)]. The diffractogram of the clay used in the composites preparation (not shown here) presents a series of reflections at 12.6, 20.0, 21.0, 25.0, and 26.8° of 2θ.[15] In the WAXS patterns of all the composites, the reflections typical of the additives (clay or TiO_2) appear together with those characteristic of the α-form (and γ-form) of the iPP [see Fig. 1(b,c)]. The iPP/TiO_2 composites shows two reflections at about 25.0 and 25.5° of 2θ [see Fig. 1(c)], which are typical from the "brookite" crystallographic form of the TiO_2.[23,24] In the iPP/TiO_2 slowly cooled composites, the γ-form gradually disappears with increasing TiO_2 amount. On the other hand, quenched composites with 10 and 30 wt % of TiO_2 (not shown here) also present a small contribution of the iPP β-form (peak at 16.1° of 2θ).[22]

The dependence of WAXS crystallinity (α_{WAXS}) on the additive content (ϕ) of the composites is shown in Figure 2(a,b) for the slowly cooled and quenched samples, respectively. In the former case (slowly cooled samples), the crystallinity of the clay composites decreases, and that of the TiO_2 increases, with increasing ϕ content [Fig. 2(a)]. However, for the quenched samples, the crystallinity increases with ϕ for both additive types [Fig. 2(b)].

From the (110) reflection, appearing at 14.09 2θ (°), the corresponding crystal size l_{110} values were derived from the expression: $l_{110} \approx k\lambda/B \cos\theta$ (Scherrer's equation), where k is equal to 0.9 for the iPP,[25] λ is equal to 0.15 nm), and B is the integral width of the reflection in radians (see Tables I and II). Instrumental broadening was negligible.

Microindentation hardness

For the slowly cooled composites, the microhardness H decreases with increasing additive content ϕ. This effect is much less pronounced for the TiO_2 composites [see Fig. 3(a)]. However, the microhardness for the quenched samples increases linearly with ϕ, irrespective of the additive used [Fig. 3(b)].

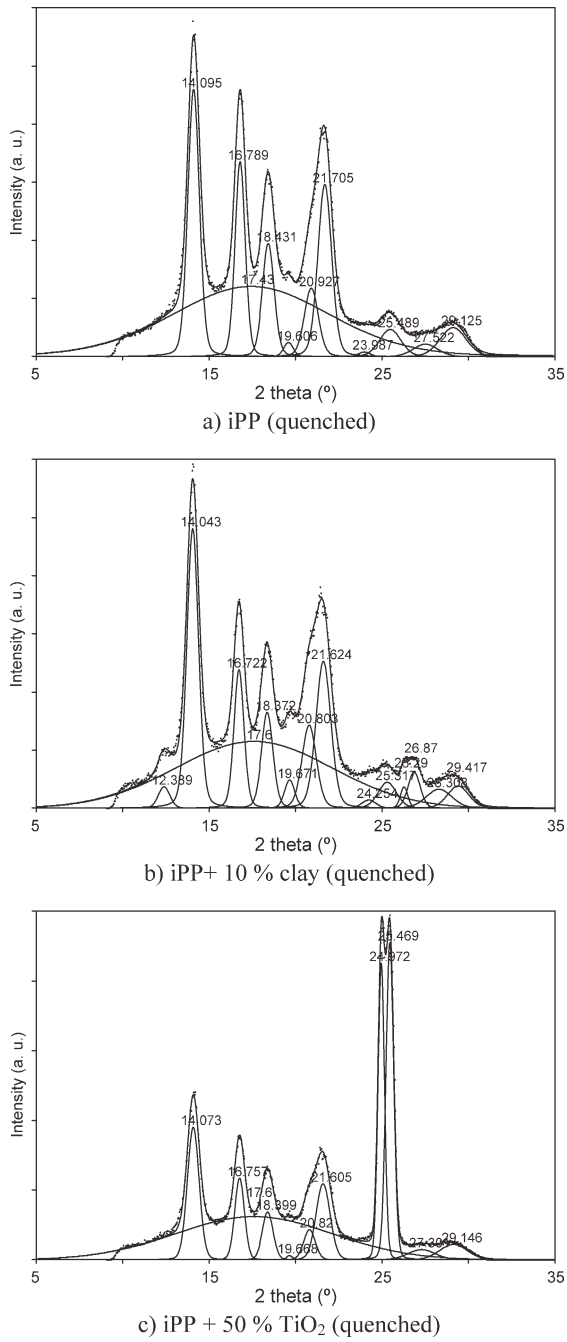

Figure 1 X-ray diffractograms of (a) iPP, and iPP with (b) 10% clay, (c) 50% TiO_2 quenched composites.

Mechanical behavior

In case of the TiO_2 quenched composites, both the tensile strength, Y_t, and the Young's modulus, E, decrease with increasing ϕ content [Fig. 4(a,b)]. However, for the clay quenched composites, the tensile strength, Y_t, decreases [Fig. 4(a)] while the

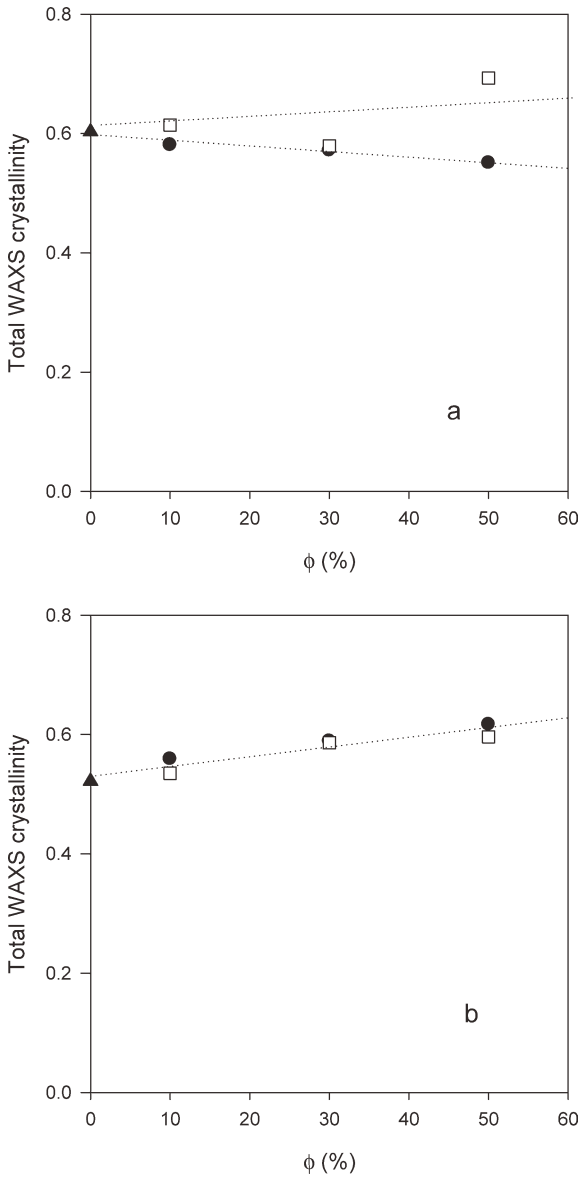

Figure 2 WAXS crystallinity as a function of the additive content ϕ for slowly cooled (a) and quenched (b) composites. ●: iPP/clay composites; □: iPP/TiO_2 composites.

Young's modulus E increases with increasing amount of clay [Fig. 4(b)].

DSC study

The DSC crystallinity (α_{DSC}) decreases linearly with the increase in ϕ for all the composites. In the slowly cooled composites, the variation is from 0.56 to 0.33. For the quenched composites, the crystallinity diminishes from 0.5 to 0.3, approximately.

In the slowly cooled composites, the melting point T_m of the iPP component (170°C) is slightly diminished by the first addition of clay or TiO_2, and after that remains practically constant (T_m values in the range 162–165°C). Quenched composites show for the iPP melting point the same value as for the pure polymer (164°C).

TABLE I
Additive Content ϕ, Crystal Thickness Values l_{110} (derived from WAXS) and l_c (derived from DSC) for the Slowly Cooled Composites: PPC (iPP/clay samples); PPT (iPP/TiO_2 samples)

Sample	ϕ	l_{110} (nm) (from WAXS)	l_c (nm) (from DSC)
PP0	0	24.0	26.6
PPC1	10	21.4	20.3
PPC2	20	–	21.9
PPC3	30	20.1	21.2
PPC4	40	–	20.6
PPC5	50	19.8	18.6
PPT1	10	23.6	22.5
PPT2	20	–	20.8
PPT3	30	21.1	21.5
PPT4	40	–	20.9
PPT5	50	21.9	20.8

The thermodynamic crystal size l_c derived for the iPP was calculated from the melting point of every sample through the well known Thomson–Gibbs equation[26]:

$$T_m = T_m^0[1 - (2\sigma_e/\Delta H_m^\infty l_c)]. \quad (1)$$

In this equation, T_m is the experimental iPP melting point (in °K), $T_m^0 = 460.7$°K is the iPP equilibrium melting point,[26] $\Delta H_m^\infty = 207.33$ J/g is the melting enthalpy for an iPP infinitely thick crystal,[26] and $\sigma_e = 100$ erg/cm^2 represents the surface free energy of the iPP crystals.[27] The l_c derived values are included in Tables I and II.

DISCUSSION

Preceding investigations have shown that the micromechanical properties of polymer composites and

TABLE II
Additive Content ϕ, Crystal Thickness Values l_{110} (derived from WAXS) and l_c (derived from DSC) for the Quenched Composites: PPC (iPP/clay samples); PPT (iPP/TiO_2 samples)

Sample	ϕ	l_{110} (nm) (from WAXS)	l_c (nm) (from DSC)
PP0Q	0	19.8	19.8
PPC1Q	10	19.6	18.9
PPC2Q	20	–	21.3
PPC3Q	30	19.9	17.0
PPC4Q	40	–	18.4
PPC5Q	50	19.3	18.3
PPT1Q	10	20.4	19.8
PPT2Q	20	–	18.8
PPT3Q	30	20.5	19.1
PPT4Q	40	–	18.9
PPT5Q	50	19.5	18.3

The letter "Q" stands for "quenched samples."

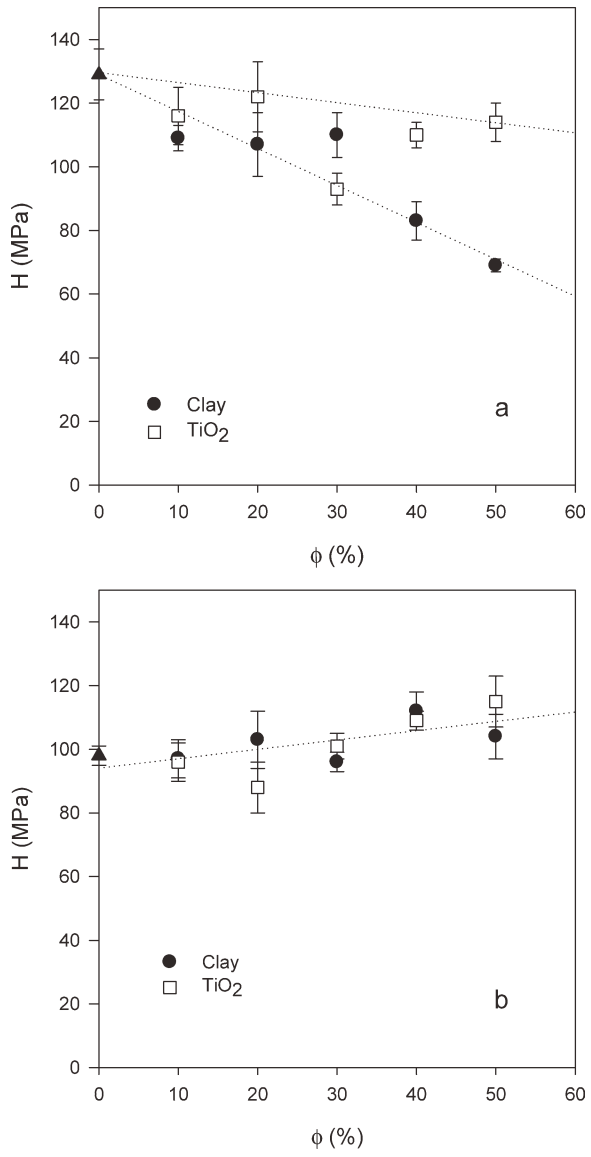

Figure 3 Microhardness H of iPP/clay and iPP/TiO_2 composites as a function of additive content ϕ for slowly cooled (a) and quenched (b) composites. Symbols as in Figure 2.

blends strongly depend on the level of crystallinity α, as well as on the nanostructural parameters (l_c).[21,28,29] Therefore, the object of this study is to try to correlate the micromechanical properties not only with the additive content and type of additive, but also most especially with the crystallinity level and nanostructural parameters.

The results for the quenched samples indicate that the crystallinity slightly increases with the additive content for both types of additive [Fig. 2(b)]. In addition, the values of l_{110} and l_c remain practically constant (see Table II). Since H is directly dependent on the crystallinity of the composites, the increasing variation of H with the additive content [Fig. 3(b)] is consistent with the results of Figure 2(b).

However, for the slowly cooled composites [Fig. 2(a)] we observe only a very small α_{WAXS} increase with ϕ for the TiO_2 additive. The composites of iPP with clay unexpectedly show a slight decrease. The l_{110} and l_c values diminish a little with the first amount of the additive, thereafter remaining practically constant (see Table I). Moreover, the hardness H of these composites clearly diminishes with increasing ϕ values, especially for the clay composites [Fig. 3(a)]. The decrease of α_{WAXS} and, consequently, of H with the additive content might be related with the difficulty of reaching a similar level of crystallinity when slowly cooling the composites. In a preceding study, we found a similar behavior for a series of reversibly crosslinked iPP/clay composites.[19] A possible explanation for this effect could be that the mobility of the iPP chains, and consequently, their crystallization capability should be restricted by the presence of an increasing amount of

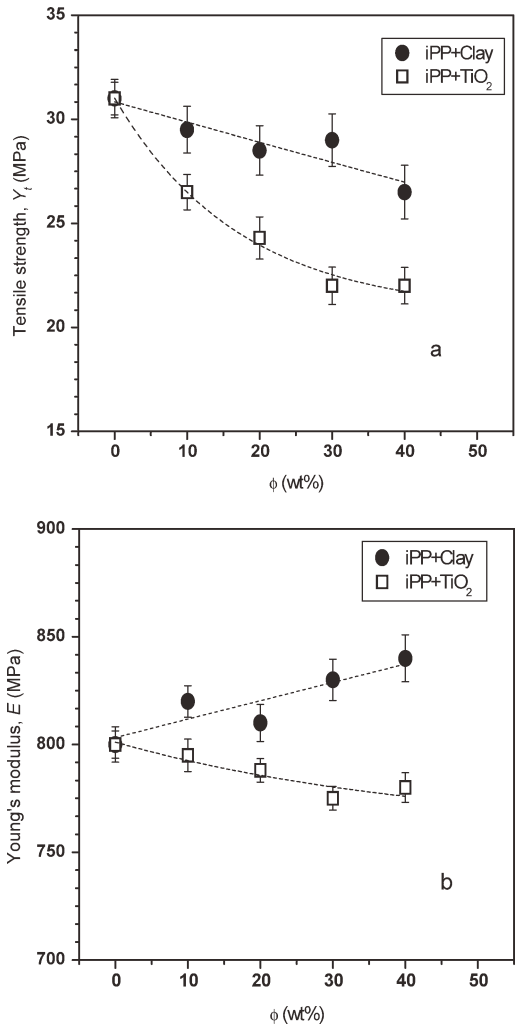

Figure 4 Plots showing the relationship between the tensile strength Y_t (a), and the Young's modulus E (b) with the additive content for the quenched composites. Symbols as in Figures 2 and 3.

clay.[19] On the other hand, nanocomposites of iPP with 5% TiO_2 nanoparticles were found to show a bimodal distribution of lamellar thickness,[30] as compared to the monomodal distribution of the pure polymer. This behavior was ascribed to the partial effect of the introduced particles that could hinder the crystallization, thus giving rise to regions with poor crystallization and regions with no hindered crystallization.

In fact, in most of the composites studied in the present work, the crystallinity of the iPP component decreases as the additive content ϕ increases. For instance, in the slowly cooled composites, α_{iPP} diminishes from 0.60 for $\phi = 0$ to 0.49 (clay composites) or 0.57 (TiO_2 composites) for $\phi = 50$. In the quenched TiO_2 composites, α_{iPP} decreases from 0.52 ($\phi = 0$) to 0.44 ($\phi = 50$). The only exception is that of the quenched clay composites, with α_{iPP} increasing from 0.52 to 0.56 when ϕ varies from 0 to 50%.

On the other hand, the hardness of the iPP component can be described, as it is known, in terms of the hardness values of its crystalline H_c and amorphous H_a phases, according to the additivity law[31]:

$$H = H_c\alpha + H_\alpha(1 - \alpha), \quad (2)$$

where α stands for the degree of crystallinity of the polymer.

Moreover, hardness of the iPP crystals H_c is related to its crystal thickness l_c through the expression[31]:

$$H_c = H_c^\infty/(1 + b/l_c), \quad (3)$$

where H_c^∞ is the hardness of an infinitely thick crystal, and the b-parameter is defined as $b = 2\sigma_e/\Delta h$.[31] In this formula, σ_e is the free surface energy and Δh is the energy required for the plastic deformation of the crystals. The σ_e value, and hence, the b-parameter value, are influenced by the degree of order at the crystals surface.[32] The blending of the iPP with increasing amounts of additive will probably originate iPP crystals with more disordered surfaces,[32] thus giving rise to smaller H_c values. In addition, it has to be taken into account the slight decrease in the iPP crystal thickness l_c occurring in the composites compared to that of the pure polymer.

Struik[33] developed a model based on the intermolecular forces between two molecules, and predicted the following relationship between the yield stress σ_e and the Young's modulus E for polymers at room temperature:

$$\sigma_e \approx E/30. \quad (4)$$

Equation (4) was successfully tested for several semicrystalline and amorphous polymers subjected to tensile experiments. In addition, in the study of a series of polyethylene PE samples with different morphologies,[34] it was found that the microhardness H and the yield stress σ_e (in tension) were related through the formula:

$$H \approx 3\sigma_e. \quad (5)$$

By combining expressions (4) and (5), the relationship $H/E \approx 0.10$ was derived for those PE samples.[34] The H and E values obtained for the quenched iPP/clay composites studied in the present work are listed in Table III. From this table, it can be seen that the average relationship between H and E derived for this set of samples is $H/E \approx 0.12$, that is, not far from the value reported in.

TABLE III
Additive Content ϕ, Hardness H Values, Young's Modulus E Values, and H/E Relationship Derived for the iPP/clay Quenched Composites

Sample	ϕ	H (MPa)	E (MPa)	H/E
PP0Q	0	98	800	0.12
PPC1Q	10	97	820	0.12
PPC2Q	20	103	810	0.13
PPC3Q	30	96	830	0.12
PPC4Q	40	112	844	0.13
PPC5Q	50	104	–	–

Unexpectedly, in case of the quenched iPP/TiO_2 composites, the values of E decrease with ϕ in contrast with the observed increase in H [see Figs. 3(b) and 4(b)]. As H is measured in compression and E is obtained from the tensile experiments, these two magnitudes might be affected differently by the degree of adhesion between the polymer and the additive, which could be, in turn, different for the clay and for the TiO_2.

The preceding results clearly indicate that the cooling process plays an important role in the structural and mechanical properties of the resulting composites. Thus, in the samples subjected to a slow cooling process, the presence of increasing amounts of clay or TiO_2 results in a crystallinity decrease or increase, respectively. The crystal thickness of the iPP crystallites in the composites slightly diminishes only with the first amount (10%) of the additive. However, in the quenched composites, the iPP crystal thickness values are almost constant for all samples, and the microhardness of the material depends only on its composition.

CONCLUSIONS

- Blending of iPP with clay, or TiO_2, through extrusion and compression molding and the subsequent cooling process, affects the level of

crystallinity of the resulting composite materials.
- The crystal thickness of the iPP in the composites is much less influenced by the blending process.
- The micromechanical and macromechanical properties of the composites depend on their composition, and also show a clear dependence on the cooling process.
- For the quenched clay composites, it has been found that the hardness H and the Young's modulus E are related by the expression $H/E \approx 0.12$.

The authors thank Dr. S. S. Funari for his technical assistance at the A2 beamline of HASYLAB.

References

1. Friedrich, K.; Fakirov, S.; Zhang, Z. Polymer Composites: From Nano-to Macroscale; Friedrich, K., Ed.; Springer, Heidelberg, 2005.
2. Åström, B. T. Manufacturing of Polymer Composites; Nelson Thornes Ltd.: United Kingdom, 2002.
3. Kausch, H. H., Ed. Advanced Thermoplasics Composites. Characterization and Processing; Carl Hanser, Munich, 1993.
4. Lee, Y. J.; Manas-Zloczower, I.; Feke, D. L. Polym Eng Sci 1995, 35, 1037.
5. Chen, X.; Shi, J.; Wang, L.; Shi, H.; Liu, Y.; Wang, L. Polym Compos 2011, 32, 177.
6. Luyt, A. S.; Molefi, J. A.; Krump, H. Polym Degrad Stab 2006, 91, 1629.
7. Zhou, Y.; Rangari, V.; Mahfuz, H.; Jeelani, S.; Mallick, P. K. Mater Sci Eng 2005, 402, 109.
8. Kumer, R. V.; Koltypin, Y.; Gedanken, A. J Appl Polym Sci 2002, 86, 160.
9. Kumer, R. V.; Koltypin, Y.; Cohen, Y. S.; Cohen, Y.; Aurbach, D.; Palchik, O.; Felner, I. J Mater Chem 2000, 10, 1125.
10. Calcagno, C. I. W.; Mariani, C. M.; Teixeira, S. R.; Mauler, R. S. Polymer 2007, 48, 966.
11. Gafur, M. A.; Nasrin, R.; Mina, M. F.; Bhuiyan, M. A. H.; Tamba, Y.; Asano, T. Polym Degrad Stab 2010, 95, 1818.
12. Wang, Y.; Wang, J. Polym Eng Sci 1999, 39, 190.
13. Chen, M.; Tian, G.; Zhang, Y.; Wan, C.; Zhang, Y. J Appl Polym Sci 2006, 100, 1889.
14. Mina, M. F.; Banu, N.; Razzak, A.; Rahman, M. J.; Gafur, M. A.; Bhuiyan, M. A. H. Polym Plast Technol Eng 2009, 48, 1275.
15. Razzak, A.; Bhuiyan, A. H. Ind J Phys 2002, 76A, 443.
16. Lei, S. G.; Hoa, S. V.; Ton-That, M.-T. Compos Sci Technol 2006, 66, 1274.
17. Mina, M. F.; Seema, S.; Matin, R.; Rahaman, M. J.; Sarker, R. B.; Gafur, M. A.; Bhuiyan, M. A. H. Polym Degrad Stab 2009, 94, 183.
18. Bhuiyan, A. H.; Mina, M. F.; Seema, S.; Khan, M. M.; Rahman, M. J.; Gafur, M. A. J Polym Res 2010, DOI 10.1007/s10965–010-9509-y.
19. Bouhelal, S.; Cagiao, M. E.; Khellaf, S.; Tabet, H.; Djellouli, B.; Benachour, D.; Baltá Calleja, F. J. J Appl Polym Sci 2010, 115, 2654.
20. Bouhelal, S.; Cagiao, M. E.; Djellouli, B.; Rong, L.; Hsiao, B. S.; Baltá Calleja, F. J. J Appl Polym Sci 2010, 117, 3262.
21. Karger-Kocsis, J., Ed. Polypropylene, Vol. 1: Structure, Blends and Composites; Chapman and Hall: London, 1995.
22. Tomota, K.; Petrykin, V.; Kobayashi, M.; Shiro, M.; Yoshimura, M.; Kakihana, M. Angew Chem Int Ed Engl 2006, 45, 2378.
23. Reyes-Coronado, D.; Rodríguez-Gattorno, G.; Espinosa-Pesqueira, M. E.; Cab, C.; de Coss, R.; Oskam, G. Nanotechnology 2008, 19, 145605.
24. Cullity, B. D.; Stock, S. R. Elements of X-ray Diffraction, 3rd ed.; Prentice Hall: NJ, 2001.
25. Wunderlich, B. Macromolecular Physics; Academic Press: New York, 1980; Vol. 3, Crystal melting, p 48.
26. Flores, A.; Aurrekoechea, J.; Gensler, R.; Kausch, H. H.; Baltá Calleja, F. J. Colloid Polym Sci 1998, 276, 786.
27. Baltá Calleja, F. J.; Fakirov, S. Microhardness of Polymers (Solid State Science Series); Cambridge University Press: Cambridge, 2000, Chapter 1, p 3 and Chapter 2, p 16.
28. Krumova, M.; Fakirov, S.; Baltá Calleja, F. J.; Evstatiev, M. J Mater Sci 1998, 33, 2857.
29. Krache, R.; Benachour, D.; Cagiao, M. E.; Baltá Calleja, F. J.; Bayer, R. K.; Tschöpe, F. Int J Polym Mater 2003, 52, 939.
30. Spieckermann, F.; Wilhelm, H.; Kerber, M.; Schafler, E.; Polt, G.; Bernstorff, S.; Addiego, F.; Zehetbauer, M. Polymer 2010, 51, 4195.
31. Flores, A.; Ania, F.; Baltá Calleja, F. J. Polymer 2009, 50, 729.
32. Baltá Calleja, F. J.; Fakirov, S. Microhardness of Polymers (Solid State Science Series); Cambridge University Press: Cambridge, 2000, Chapter 4, p 101 and Chapter 7, p 205.
33. Struik, L. C. E. J Non-Cryst Solids 1991, 131, 395.
34. Flores, A.; Baltá Calleja, F. J.; Attenburrow, G. E.; Basset, D. C. Polymer 2000, 41, 5431.